Chapter 18
Measurement of CKM Angle ϕ_3 Using $B^{\pm} \to D(K^0_S\pi^+\pi^-\pi^0)K^{\pm}$ Decays at Belle

P. K. Resmi, James F. Libby, and K. Trabelsi

Abstract The CKM angle ϕ_3 can be determined in a theoretically clean way as it is accessible via the tree-level decays, $B^{\pm} \to DK^{\pm}$. The current uncertainty on ϕ_3 is significantly larger than that of the standard model (SM) prediction. A more precise measurement of ϕ_3 is crucial for testing the SM description of CP violation and probing for new physics effects. The statistical uncertainty can be reduced if information from additional D meson final states is included, which in practice means new three and four-body decay modes. Here, we measure ϕ_3 with $B^{\pm} \to D(K^0_S\pi^+\pi^-\pi^0)K^{\pm}$ decays using a data sample corresponding to an integrated luminosity of 711 fb^{-1} collected with the Belle detector at KEKB asymmetric e^+e^- collider. This four-body D final state has a large branching fraction of 5.2% and the phase space is rich with different resonance substructures. We adopt a model-independent method to estimate ϕ_3 by studying various regions of the phase space. The D decay strong-phase information is obtained from the quantum-correlated D meson pairs produced at CLEO-c.

18.1 Introduction

The current best measurement of the CKM [1, 2] angle ϕ_3, combining all the results from different experiments, is $(73.5^{+4.2}_{-5.1})^\circ$ [3]. This large uncertainty is due to the small branching fractions of the decays sensitive to ϕ_3. The value of ϕ_3 estimated indirectly from other parameters of the unitarity triangle is $(65.3^{+1.0}_{-2.5})^\circ$ [3]. Any disagreement between these results could imply that there is new physics beyond the standard model (SM). But a comparison would be meaningful only if the associated uncertainties are

P. K. Resmi, J. F. Libby, and K. Trabelsi on behalf of Belle Collaboration.

P. K. Resmi (✉) · J. F. Libby
Indian Institute of Technology Madras, Chennai, India
e-mail: resmipk@physics.iitm.ac.in

K. Trabelsi
Laboratorie de L'accélérateur Linéaire, Orsay, France

P. K. Behera et al. (eds.), *XXIII DAE High Energy Physics Symposium*,
Springer Proceedings in Physics 261,
https://doi.org/10.1007/978-981-33-4408-2_18

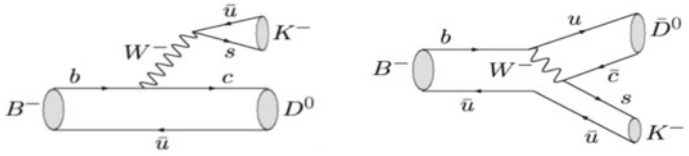

Fig. 18.1 Color-favored (left) and color-suppressed (right) $B^- \to DK^-$ processes

comparable. Thus, an improved measurement of ϕ_3 is essential for testing the SM description of *CP* violation. The color-favored $B^- \to D^0 K^-$ and color-suppressed $B^- \to \overline{D^0} K^-$ decays, where D indicates a neutral charm meson reconstructed in a final state common to both D^0 and $\overline{D^0}$, provide *CP*-violating observables, that are sensitive to ϕ_3. Here and elsewhere in this paper, charge conjugation of final states is implied unless explicitly stated otherwise. The Feynman diagrams are shown in Fig. 18.1. These are tree-level decays and hence the theoretical uncertainty is negligible ($\mathcal{O}(10^{-7})$) [4].

If the amplitude for the color-favored decay is $A_{\text{fav}} = A$, then the color-suppressed one can be written as $A_{\text{sup}} = A r_B e^{i(\delta_B - \phi_3)}$, where δ_B is the strong-phase difference between the decay processes, and

$$r_B = \frac{|\, A_{\text{sup}} \,|}{|\, A_{\text{fav}} \,|}. \tag{18.1}$$

The statistical uncertainty on ϕ_3 is proportional to r_B. For $B^+ \to DK^+$ decays, $r_B \sim 0.1$, whereas for $B^+ \to D\pi^+$, it is 0.005. Though $B^+ \to D\pi^+$ decays are not very sensitive to r_B and ϕ_3, they serve as excellent control sample modes for signal extraction procedure in $B^+ \to DK^+$ due to their similar kinematics. This also helps in determining the cross-feed background due to the misidentification of kaons and pions from data.

The limitations on the current ϕ_3 measurements due to statistical precision can be reduced by exploring more and more D final states. Here, we study the four-body self-conjugate state, $D \to K^0_S \pi^+ \pi^- \pi^0$. This decay mode has a branching fraction of 5.2% [5], which is almost twice that of $D \to K^0_S \pi^+ \pi^-$, the dominant multi-body D final state used to determine ϕ_3 [6, 7]. This decay proceeds via interesting resonance substructures like $K^0_S \omega$, $K^* \rho$, etc., thus facilitating a model-independent extraction of ϕ_3 by studying the D phase space regions. We present the expected results from $B^+ \to DK^+$ decays by analyzing simulated samples and preliminary results obtained from the $B^+ \to D\pi^+$ data sample, i.e., the calibration mode.

18.2 Formalism to Measure ϕ_3 Sensitive Parameters

The methods to determine ϕ_3 vary according to the D meson final state under consideration. When it is a multibody self-conjugate state, there are two methods: model-dependent and model-independent. In the model-dependent method, the D amplitudes are fitted to a model corresponding to the intermediate resonances. The model assumptions cause large uncertainties that could limit the precision of the ϕ_3 measurement. The model-independent approach provides measurements of CP violating asymmetries made in independent regions of the D phase space [8, 9]. This binning reduces the statistical precision, but the uncertainty due to model assumptions are no longer present as the average strong-phase measurements are used. This analysis follows the model-independent method.

The D phase space is binned into regions with differing strong phases, which allows ϕ_3 to be determined from a single channel in a model-independent manner. The signal yield for $B^{\pm} \to DK^{\pm}$ decays in each bin is given as

$$\Gamma_i^{\pm} \propto K_i + r_B^2 \overline{K_i} + 2\sqrt{K_i \overline{K_i}}(c_i x_{\pm} \mp s_i y_{\pm}), \tag{18.2}$$

where $x_{\pm} = r_B \cos(\delta_B \pm \phi_3)$ and $y_{\pm} = r_B \sin(\delta_B \pm \phi_3)$. The $x_{\pm}$ and $y_{\pm}$ parameters, that are sensitive to ϕ_3, can be obtained when the phase space is divided into three or more bins. Here, K_i and $\overline{K_i}$ are the fraction of flavor-tagged D^0 and $\overline{D^0}$ events in the i^{th} bin, respectively, which can be estimated from $D^{*+} \to D^0\pi^+$ decays with good precision due to their large sample size. The parameters c_i and s_i are the amplitude-weighted average of the cosine and sine of the strong-phase difference between D^0 and $\overline{D^0}$ over the i^{th} bin; these parameters need to be determined at a charm factory experiment like CLEO-c or BESIII, where the quantum-entangled $D^0\overline{D^0}$ pairs are produced via $e^+e^- \to \psi(3770) \to D^0\bar{D}^0$ [10]. The values of c_i and s_i parameters for $D \to K^0_S\pi^+\pi^-\pi^0$ decays as well as the binning scheme to divide the D phase space reported in [11] are used in this analysis.

18.3 Data Samples and Event Selection

The e^+e^- collision data sample at a center-of-mass energy corresponding to the pole of the $\Upsilon(4S)$ resonance collected by the Belle detector [12, 13] is used in this analysis. It corresponds to an integrated luminosity of 711 fb^{-1} and contains 772×10^6 $B\overline{B}$ pairs. The Belle detector is located at the interaction point (IP) of KEKB asymmetric e^+e^- collider [14]. A detailed description of the Belle detector is given in [12, 13]. Monte Carlo (MC) samples are used to optimize the selection criteria, determine the efficiencies, and identify various sources of background.

We reconstruct $B^+ \to DK^+$ and $B^+ \to D\pi^+$ decays in which the D decays to the four-body final state of $K^0_S\pi^+\pi^-\pi^0$. The decays $D^{*+} \to D\pi^+$ produced via the $e^+e^- \to c\bar{c}$ continuum process are also selected to measure the K_i and $\overline{K_i}$ parame-

ters. We select the charged particle candidates produced within 0.5 cm and ± 3.0 cm of the IP in perpendicular and parallel directions to the z-axis, respectively, where the z-axis is defined to be opposite to the e^+ beam direction. These tracks are then identified as kaons or pions with the help of the particle identification system at Belle [12]. We reconstruct the K^0_S candidates from two oppositely charged pion tracks. The invariant mass of these pion candidates is required to be within $\pm 3\sigma$ of the nominal K^0_S mass [5], where σ is the mass resolution. The background due to random combinations of pions is reduced with the help of a neural network [15] based selection with 87% efficiency [16].

We reconstruct π^0 candidates from a pair of photons detected in the electromagnetic calorimeter (ECL). The π^0 candidates within the diphoton invariant mass range 0.119–0.148 GeV/c^2 are retained. The photon energy thresholds are optimized separately for candidates detected in the barrel, forward endcap, and backward endcap regions of the ECL. Furthermore, kinematic constraints are applied to K^0_S, π^0, and D invariant masses and decay vertices. This improves the energy and momentum resolution of the B candidates and the invariant masses used to divide the D phase space into bins.

While reconstructing $D^{*+} \to D\pi^+$ decays, it is required that the accompanying pion has at least one hit in the silicon vertex detector. This pion carries a small fraction of the momentum due to the limited phase space of the decay and hence is known as a slow pion. The D meson momentum in the laboratory frame is chosen to be between 1–4 GeV/c so that it matches to that in $B^+ \to Dh^+ (h = K, \pi)$ sample. The signal candidates are identified by the kinematic variables M_D, the invariant mass of D candidate and ΔM, the difference in the invariant masses of D^* and D candidates. We retain events that satisfy the criteria, $1.80 < M_D < 1.95$ GeV/c^2 and $\Delta M < 0.15$ GeV/c^2. A kinematic constraint is applied so that the D and π candidates come from the common vertex position. When there are more than one candidate in an event, the one with the smallest χ^2 value from the D^* vertex fit is retained for further analysis. The overall selection efficiency is 3.7%.

The B meson candidates are reconstructed by combining a D candidate with a charged kaon or pion track. Events with D meson invariant mass in the range 1.835–1.890 GeV/c^2 are selected. The kinematic variables energy difference ΔE and beam constrained mass $M_{\rm bc}$ are used to identify the signal candidates. They are defined as $\Delta E = E_B - E_{\rm beam}$ and $M_{\rm bc} = c^{-2}\sqrt{E^2_{\rm beam} - |\mathbf{p}_B|^2 c^2}$, where E_B and $\mathbf{p}_B$ are the energy and momentum of the B candidate and $E_{\rm beam}$ is the beam energy in the center-of-mass frame. The candidates that satisfy the criteria $M_{\rm bc} > 5.27$ GeV/c^2 and $-0.13 < \Delta E < 0.30$ GeV are selected. In events with more than one candidate, the candidate with the smallest value of $(\frac{M_{\rm bc} - M_B^{PDG}}{\sigma_{M_{\rm bc}}})^2 + (\frac{M_D - M_D^{PDG}}{\sigma_{M_D}})^2 + (\frac{M_{\pi^0} - M_{\pi^0}^{PDG}}{\sigma_{M_{\pi^0}}})^2$ is retained. Here, the masses $M_i^{\rm PDG}$ are those reported by the Particle Data Group in [5] and the resolutions $\sigma_{M_{\rm bc}}$, σ_{M_D} and $\sigma_{M_{\pi^0}}$ are obtained from MC simulated samples of signal events.

The main source of background is from $e^+e^- \to q\bar{q}$, $q = u, d, s, c$ continuum processes, and these are suppressed by exploiting the difference in their event topol-

ogy to that of $B\overline{B}$ events. The continuum events are jet-like in nature and $B\overline{B}$ events have a spherical topology. These events are separated with the help of a neural-network-based algorithm [15]. We require the neural network output to be greater than -0.6, which reduces the continuum background by 67% at the cost of 5% signal loss. The overall selection efficiency is 4.7 and 5.3% for $B^+ \to DK^+$ and $B^+ \to D\pi^+$ modes, respectively.

18.4 Determination of K_i and $\overline{K_i}$

The K_i and $\overline{K_i}$ parameters indicate the fraction of D^0 and $\overline{D^0}$ events in each D phase space bin. They are measured from the $D^{*+} \to D\pi^+$ sample; the charge of the pion determines the flavor of the D meson. The signal yield is obtained from a two-dimensional extended maximum-likelihood fit to M_D and ΔM distributions independently in each bin. Appropriate probability density functions (PDF) are used to model the distributions. A quadratic correlation between M_D and ΔM is taken into account for the signal component. The yields along with K_i and $\overline{K_i}$ values are given in Table 18.1.

18.5 Signal Extraction in $B^+ \to Dh^+$ Sample

The signal yield in each D phase space bin is determined from a two-dimensional extended maximum-likelihood fit to ΔE and neural network output (NB). The latter is transformed as

$$NB' = \log\left(\frac{NB - NB_{\text{low}}}{NB_{\text{high}} - NB}\right), \tag{18.3}$$

Table 18.1 D^0 and $\overline{D^0}$ yield in each bin of D phase space along with K_i and $\overline{K_i}$ values measured in D^* tagged data sample

Bin no.	N_{D^0}	$N_{\overline{D^0}}$	K_i	$\overline{K_i}$
1	51048±282	50254±280	0.2229±0.0008	0.2249±0.0008
2	137245±535	58222±382	0.4410±0.0009	0.1871±0.0007
3	31027±297	105147±476	0.0954±0.0005	0.3481±0.0009
4	24203±280	16718±246	0.0726±0.0005	0.0478±0.0004
5	13517±220	20023±255	0.0371±0.0003	0.0611±0.0004
6	21278±269	20721±267	0.0672±0.0005	0.0679±0.0005
7	15784±221	13839±209	0.0403±0.0004	0.0394±0.0004
8	6270±148	7744±164	0.0165±0.0002	0.0183±0.0002
9	6849±193	6698±192	0.0070±0.0002	0.0054±0.0001

where $NB_{\text{low}} = -0.6$ and $NB_{\text{high}} \approx 1.0$ are the minimum and maximum values of NB in the sample, respectively. The three background components are continuum background, combinatorial $B\overline{B}$ background due to final state particles from both the B mesons and cross-feed peaking background due to the misidentification of a kaon as a pion or *vice versa*.

The sum of a Crystal Ball (CB) [17] function and two Gaussian functions with a common mean is used as the PDF to model the ΔE signal component in both the B samples. The sum of a Gaussian and an asymmetric Gaussian with different mean values is used to parametrize the PDF that describes the NB' signal component. The continuum background distribution in ΔE is modeled with a first-order Chebyshev polynomial and that in NB' is described by the sum of two Gaussian PDFs with different mean values. The ΔE distribution of random $B\overline{B}$ background in $B^+ \to D\pi^+$ is described by an exponential function. There is a small peaking structure due to misreconstructed π^0 events and this is modeled by a CB function. A first-order Chebyshev polynomial is added to the above two PDFs in the case of $B^+ \to DK^+$ decays. The NB' distribution for both the samples are modeled by an asymmetric Gaussian function. The cross-feed peaking background in ΔE is modeled with the sum of three Gaussian functions, whereas the signal PDF itself is used for the NB' distribution. The fit projections in $B^+ \to DK^+$ MC sample are shown in Fig. 18.2. These are signal-enhanced projections with events in the signal region of the other variable, where the signal regions are defined as $|\Delta E| < 0.05$ GeV and $0 < NB' < 12$.

The ϕ_3 sensitive parameters are determined directly from the fit by expressing the signal yield as in (18.2). The K_i and $\overline{K_i}$ values along with the c_i and s_i measurements

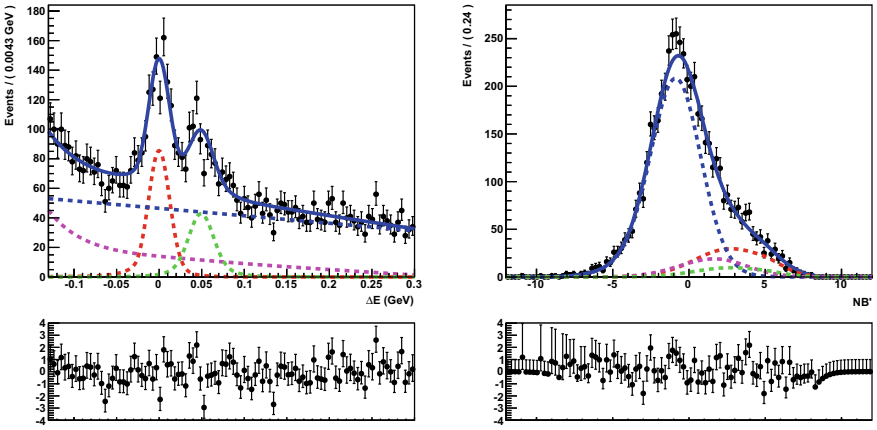

Fig. 18.2 Signal-enhanced fit projections of ΔE (left) and NB' (right) for $B^{\pm} \to DK^{\pm}$ MC sample having equivalent luminosity as that of full data sample collected by Belle. The black points with the error bar are the data and the solid blue curve is the total fit. The dotted red, blue, magenta, and green curves represent the signal, continuum, random $B\overline{B}$ backgrounds, and cross-feed peaking background components, respectively. The pull between the data and the fit are shown for both the projections

Table 18.2 Preliminary results of $x_{\pm}$and $y_{\pm}$ parameters from $B^{\pm} \to D\pi^{\pm}$ data sample. The first uncertainty is statistical, second is systematic and the third one is due to the uncertainty on the c_i, s_i measurements

Parameter	Result
$x_{+}^{D\pi}$	$0.04 \pm 0.03 \pm 0.03 \pm 0.01$
$y_{+}^{D\pi}$	$0.06^{+0.08}_{-0.20} \pm 0.10^{+0.07}_{-0.03}$
$x_{-}^{D\pi}$	$0.01 \pm 0.02^{+0.02}_{-0.03} \pm 0.02$
$y_{-}^{D\pi}$	$-0.02 \pm 0.06^{+0.03}_{-0.04} \pm 0.06$

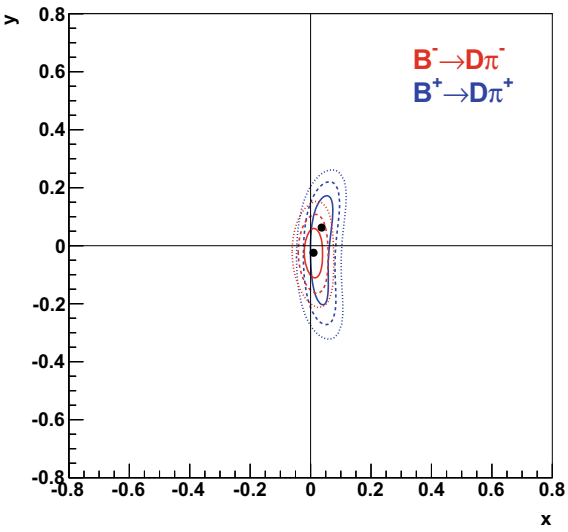

Fig. 18.3 One (solid line), two (dashed line), and three (dotted line) standard deviation likelihood contours for the $(x_{\pm}, y_{\pm})$ parameters for $B^{\pm} \to D\pi^{\pm}$ data sample

reported in [11] are used as input parameters. Efficiency corrections are applied and the effect of migration of events between the bins due to finite momentum resolution is also taken into account. The preliminary results obtained from $B^{+} \to D\pi^{+}$ data sample are summarized in Table 18.2. The dominant source of systematic uncertainty is the size of the signal MC sample used for estimating the efficiency and the extent of migration between the bins. The statistical likelihood contour is given in Fig. 18.3.

18.6 Summary

A precise measurement of the CKM angle ϕ_3 is essential to establish the SM description of CP violation. Here, we present the feasibility of $D \to K^0_S\pi^+\pi^-\pi^0$ final state to do so in $B^{+} \to DK^{+}$ decays. This is the first attempt to analyze this particular decay mode. The signal extraction procedure is established in an MC sample, as

well as $B^+ \to D\pi^+$ data sample, the calibration mode. MC predictions estimate the statistical uncertainty on $x_\pm$, $y_\pm$ in $B^+ \to DK^+$ to be 0.08 and 0.17, respectively.

An improved measurement is possible once an amplitude model for $D^0 \to K^0_S\pi^+\pi^-\pi^0$ is available to guide the binning of the phase space such that maximum sensitivity to ϕ_3 is obtained. Furthermore, a more precise measurement of c_i, s_i parameters could be performed with a larger sample of $e^+e^- \to \psi(3770)$ data that has been collected by BESIII, thus reducing the systematic uncertainty. The Belle II detector is expected to collect about 50 times larger B sample. Thus, the improved binning combined with the larger B sample make $B^+ \to D(K^0_S\pi^+\pi^-\pi^0)K^+$ a promising addition to the set of modes to be used to determine ϕ_3 to a precision of 1–2° [18].

References

1. N. Cabibbo, Unitary symmetry and leptonic decays. Phys. Rev. Lett. **10**, 531 (1963)
2. M. Kobayashi, T. Maskawa, CP violation in the renormalizable theory of weak interaction. Prog. Theor. Phys. **49**, 652 (1973)
3. Y. Amhis et al., (Heavy Flavor Averaging Group Collaboration): averages of b-hadron, c-hadron and τ-lepton properties as of November 2016. Eur. Phys. J **C77**, 895 (2017)
4. J. Brod, J. Zupan, The ultimate theoretical error on gamma from $B \to DK$ decays. J. High. Energ. Phys. **01**, 051 (2014)
5. M. Tanabashi et al., (Particle Data Group Collaboration): review of particle physics. Phys. Rev. D. **98**, 030001 (2018)
6. H. Aihara et al., (Belle Collaboration): first measurement of ϕ_3 with a model-independent Dalitz plot analysis of $B^\pm \to DK^\pm$, $D \to K^0_S\pi^+\pi^-$ decay. Phys. Rev. D **85**, 112014 (2012)
7. A. Poluektov et al., (Belle Collaboration): evidence for direct CP violation in the decay $B^\pm \to D^{(*)}K^\pm$, $D \to K^0_S\pi^+\pi^-$ and measurement of the CKM phase ϕ_3. Phys. Rev. D **81**, 112002 (2010)
8. A. Giri, Y. Grossman, A. Soffer, J. Zupan, Determining γ using $B^\pm \to DK^\pm$ with multibody D decays. Phys. Rev. D **63**, 054018 (2003)
9. A. Bondar, Proceedings of BINP special analysis meeting on Dalitz analysis, 2002 (unpublished). A. Giri, Y. Grossman, A. Soffer, J. Zupan, Determining γ using $B^\pm \to DK^\pm$ with multibody D decays. Phys. Rev. D **63**, 054018 (2003)
10. P.K. Resmi, Input from the charm threshold for the measurement of γ. arXiv:1810.00836 [hep-ex]
11. P.K. Resmi et al., Quantum-correlated measurements of $D \to K^0_S\pi^+\pi^-\pi^0$ decays and consequences for the determination of the CKM angle γ. J. High. Energ. Phys. **01**, 82 (2018)
12. A. Abashian et al., (Belle Collaboration): The Belle Detector. Nucl. Instrum. Methods Phys. Res. A **479**, 117 (2002)
13. J. Brodzicka et al., (Belle Collaboration): physics achievements from the belle experiment. Prog. Theor. Exp. Phys. **2012**, 04D001 (2012)
14. S. Kurokawa, E. Kikutani, Overview of the KEKB accelerators. Nucl. Instr. Meth. A **499**, 1 (2003). and other papers included in this volume
15. M. Feindt, U. Kerzel, The NeuroBayes neural network package. Nucl. Instrum. Methods Phys. Res. A **559**, 190 (2006)
16. H. Nakano, Search for new physics by a time-dependent CP violation analysis of the decay $B \to K_S\eta\gamma$ using the Belle detector, Ph.D. Thesis, Tohoku University, 2014, Chap. 4 (unpublished)

17. Skwarnicki, T.: A study of the radiative cascade transitions between the Υ and Υ' resonances, Ph.D thesis (Appendix E), DESY F31-86-02 (1986)
18. E. Kou, P. Urquijo, The Belle II collaboration, and The B2TiP theory community. *The Belle II Physics Book*. arXiv:1808.10567